Prototype of Robotic Ankle-Foot Prosthesis with Active Damping Using Magnetorheological Fluids

Oscar Arteaga, Julio Escorza, Ismael Medina, Richard Navas, Katherine Amores, and Jonathan J. Morales
Departamento de Ciencias de la Energía y Mecánica, Universidad de las Fuerzas Armadas ESPE, Sangolquí, Ecuador
Email: obarteaga@espe.edu.ec, {jdescorza, iamedina2, rfnavas1, fkamores, jjmorales7}@espe.edu.ec

***Abstract*— When an amputee walks around wearing a transtibial prosthesis that does not have adequate range of motion and cushioning, the person will have a very irregular gait. For this reason, this project is aimed at the design and implementation of an ankle and foot prosthesis, which takes advantage of technological advances, uses intelligent materials such as magnetorheological fluids (MRF) and applies computer processes to develop a prototype that guarantees a harmonious and functional gait without neglecting the aesthetic aspect; based on the study of the anatomy, biomechanics and locomotion of the lower limb, in order to provide a natural movement. A hybrid magnetorheological system was designed, equipped with a torsion limiting mechanism that emulates the movement of the ankle and foot that occurs in the sagittal plane, controlling the damping, rotation and stability, through a system that generates and controls the magnetic field that is applied to the MRF, providing greater adaptability to the patient. Tests have shown that the prosthesis meets the design requirements, as the electric actuator is positioned in such a way that the first contact with the floor is made only with the heel of the prosthesis, then the MR fluid damper absorbs the impact and finally the electric actuator gives the necessary impulse to complete the next step. The prototype is capable of replicating the angle and torsion patterns of the human ankle, for a stride speed of up to 2.8 m/s.**

***Index Terms*—ankle prosthesis, foot prosthesis, MRF fluids, active damping**

I. Introduction

Amputation is a surgical procedure that causes an irreversible change in the person undergoing the procedure. Lower limb amputation involves new biomechanical gait and load patterns, with the risk of overload injuries [1]. The need to satisfy the growing demand for rehabilitation services and to provide an accurate and timely response to the conditions that affect motor performance implies the integration of different clinical and engineering disciplines that provide integral and lasting solutions to the complex problems that involve the human gait cycle [2] [3].

With all the technological advances, the aim is to develop a prosthesis capable of correctly emulating the normal gait cycle. Exploiting current technological advances, it is intended to develop an ankle-foot prosthesis that is capable of correctly emulating the normal human gait cycle, by using intelligent materials such as magnetorheological fluids and new control strategies that include hybrid controllers that use EMG electromyography signals, non-linear PD-PID controllers, intelligent control (neural networks, genetic algorithms, fuzzy logic and expert systems), artificial intelligence and control based on the level of coordination [4] [5].

Linear actuators were also used to modulate the response of a joint, due to the advantages it offers in terms of efficiency, adjustability and speed of response. These systems are embedded in the prosthesis and electronically adjust ankle and foot flexion or extension according to the requirements of the gait cycle through control valves [5]. These intelligent prostheses provide amputees with the strength required to perform normal movements and facilitate walking activity. However, motorized prosthetics use batteries that tend to be bulky and expensive, which is a disadvantage [6] [7] [8].

Today, several researchers are developing prostheses that help people walk easily and prevent damage to their health. Therefore, the study of MRF is important to determine their properties as the magnetic field varies, and thus predict their behavior within the prototype developed, so as to ensure a range of motion and level of damping according to the activity performed by the amputee, thus contributing to the design of an intelligent and reliable prosthesis [9] [10] [11].

II. Design and Implementation of the Protest Prototype

A. Systematization of Variables.

Because the height of the person who will use the prosthesis is necessary to determine the efforts that the different components of the prototype must support, it was decided to design an ankle and foot prosthesis for an adult man of 1.75 meters in height and average weight F_S= 69 kg (50th percentile male). The medical argument that the ideal length for amputations below the knee corresponds to 0.12 meters [1] was also considered, as shown in Fig. 1. Therefore, there is 0.383 meters of leg length that must be replaced by the prosthesis. This leg length has an average weight of 3.06 kg, which represents

Manuscript received October 1, 2018; revised July 15, 2019.

doi: 10.18178/ijmerr.8.5.753-758

the maximum weight that the prototype prosthesis can have to compensate for the weight of the amputated foot.

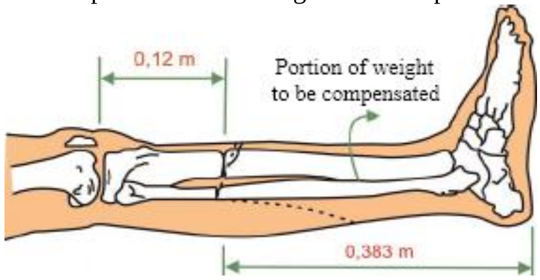

Figure 1. Amputation level diagram.

For this research, the foot was analyzed as the most distant link from the lower limb and the structural base of the locomotor apparatus [12], an argument that helped to simplify the analysis of forces present during take-off and heel contact, resulting in an ideal design according to a normal gait cycle of a person. From the mechanics of the foot and the static analysis of the force system shown in Fig. 2, the tensile force, F_T=989 N, exerted by the gastrocnemius and soleus muscles in the heel bone through the Achilles tendon, and the force of reaction, F_{RA}=1515 N, of the ankle joint applied by the tibia in the felling dome are determined.

Figure 2. Synthesis of the analysis of forces.

B. Design of the Damping System

In order to provide an adequate damping that responds in real time to the impact forces that occur during each of the phases of the gait cycle and to the gait conditions in the different activities performed by the amputee, it was decided to use LORD's MRF-140CG fluid which has a density of 3740 kg/m^3 and a viscosity of 0.28 Pa*s [13]. To characterize the MRF and determine its rheological properties at different magnetic field strengths (*H*), a rotational rheometer MCR-501 (Anton Paar Physica) equipped with a magnetorheological cell MRD-70/1Text was used. From the data obtained in the tests, Fig. 3, it was determined that MRF-140CG behaves like a Bingham plastic, evidenced by a variable shear stress [14]. Fig. 3 shows that in the absence of a magnetic field the MRF has a maximum shear stress of 440.9 Pa at 20 ℃, while under the action of a magnetic field the MRF reaches a maximum shear stress of 41,12 kPa at 800 mT and 20 ℃.

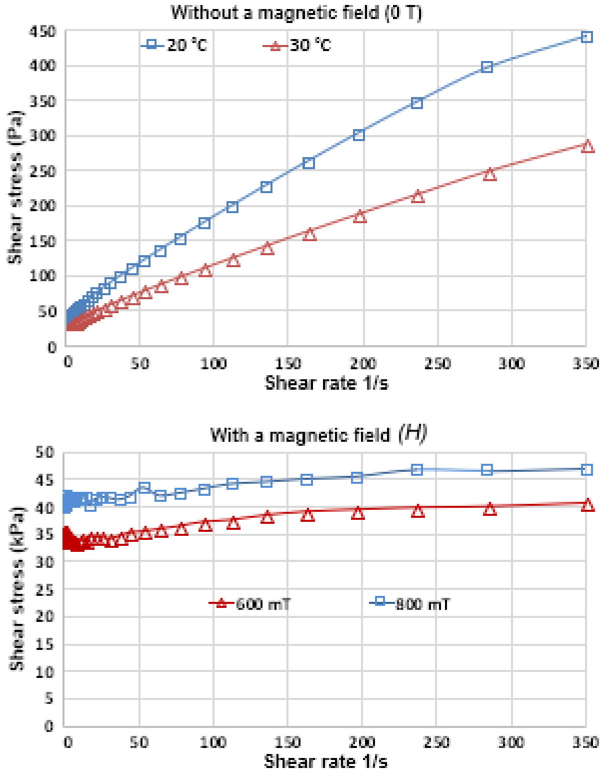

Figure 3. Behavior of MRF-140CG fluid.

For the MR fluid damper design, it was considered that the fluid operates under the valve mode with direct cut, known as parallel plate mode [15], shown in Fig. 4, where the intensity of the applied magnetic field allows to regulate the flow of fluid from one chamber to another inside the cylinder. In addition, the principle of a single-tube cylinder was used. The MR fluid damper is represented by a spring-mass system where must consider many factors in order to develop an effective valve, such as: the mass (*m*) of the body; the rigidity (*k*) of the actuator; the coefficient of viscous damping (*c*) and the force *F*(t) applied (Fig. 4).

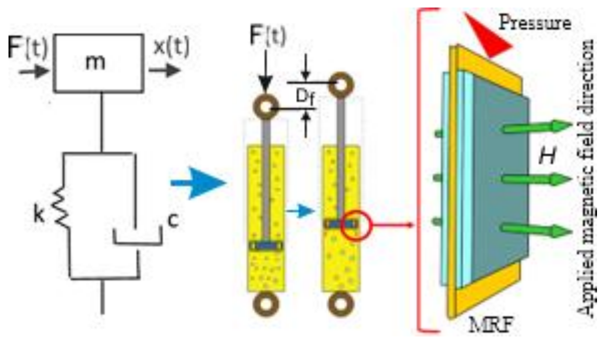

Figure 4. Mass-spring of a MR fluid damper.

Under the applied force *F*(t), the damper develops a total resistance force F_{RT} (1) composed of the controllable force $F_{\tau o}$ due to the shear stress dependent on the field (2) and the uncontrollable force F_η due to the viscosity of the fluid (3) independent of the field and the friction produced [15].

$$F_{RT} = F_{\tau_0} + (F_n + F_f) \quad (1)$$

$$F_{\tau_0} = \left(2.07 + \frac{12Q_n}{12Q_n + 0.4wh^2\tau_0}\right)\frac{\tau_0 L A_p}{h} \quad (2)$$

$$F_n = \left(1 + \frac{whv_0}{2Q}\right)\frac{12nQLA_p}{wh^3} \quad (3)$$

Another important aspect of the damper design is to determine the maximum stroke Df that the piston should travel during the entire gait cycle. As shown in Fig. 5, this stroke is calculated from the length Lp, which varies according to the different angles that the ankle and leg form during the support phase of the gait cycle (from 15° to -10°). From Fig. 5, it is determined that for a normal walk Df =15 mm. However, it was considered to increase the stroke of the piston to 30 mm, with the aim of providing a greater range of damping in extreme operating conditions of the prosthesis, such as the case in which the amputee wishes to run or jump [16].

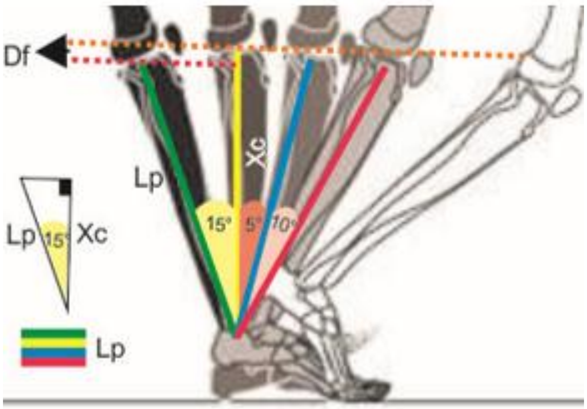

Figure 5. Determination of the cylinder stroke MR

In order for the complete piston stroke to take place in the time it takes to take a step in a normal walk (approximately 1.0 seconds), the average piston rod speed is vo=0.03 m/s, generating a flow of fluid $Q=2.88*10^{-5}$ m^3/s, for a cylinder with an internal diameter of D=35 mm and a gap h=0.35 mm. By applying (1), (2) and (3), we obtain the forces F_{RT} = 559.2 N, the controllable force $F\tau o$ = 221.0 N and the uncontrollable force $F\eta$ = 338.1 N. From Fn, the length of the magnetic pole L is calculated, resulting in 20 mm. However, in order to improve the effectiveness of the magnetic pole it is divided into 4 sections of 5 mm length each to increase the cutting areas, involving greater difficulty for the passage of MRF-140CG fluid.

To design the shank, because the power cables must be independently insulated, a hollow shank with an internal diameter of 4 mm is assumed, then the required outer diameter is calculated to prevent it from bending due to the F_{RT} compression force, using Johnson's short column equation, resulting in 10 mm [17] [18]. As for the spring, it has a maximum length of 50 mm and an internal diameter of 18 mm, so a 25 mm diameter wire with 6 coils and a pitch of 7 mm is chosen. The design result is shown in Fig. 6.

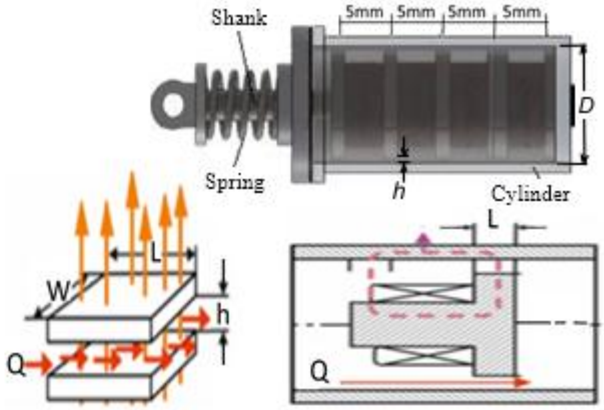

Figure 6. MR fluid damper working in mode plate-parallel.

C. *Design of the Electromagnet.*

To generate the magnetic field that allows the saturation of the MRF-140CG fluid inside the damper, the design of an electromagnet based on the solenoid principle was proposed, where the field lines are directed between the North and South poles cutting the fluid perpendicular to the direction of movement, as shown in Fig. 7. The field produced by the solenoids distributed equidistantly on the piston plunger tends to generate a magnetic field perpendicular to the direction of the fluid, with the greatest intensity being observed deepening inside it.

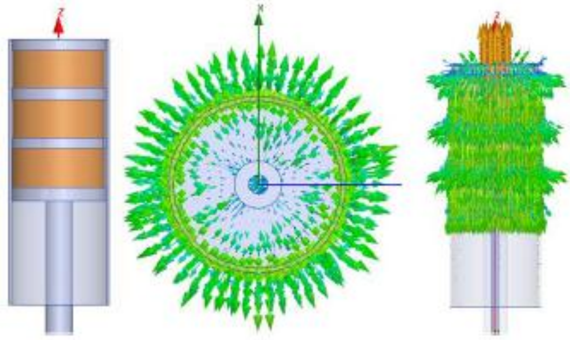

Figure 7. Distribution of magnetic fields.

Therefore, three coils are created, due to the number of sections of the magnetic pole; thus three 14 mm long coils are available connected in series, in order to create opposite directions and maintain a constant field during convergence. The number of waits (4) for each coil is 22 and the number of layers (5) is 15, which is intended to intensify the lines of the internal field. With the calculated parameters the theoretical magnetic induction inside the solenoid (6) is identified, as well as in the fluid cutting area (7).

$$N = \frac{L_s}{D_{AL}} \quad (4)$$

$$N_C = \frac{D_{tb} - D_{vástago}}{2(D_{cable})} \quad (5)$$

$$B = \frac{u_0 u_r N_i}{L_s} * N_C \quad (6)$$

$$B_X = \frac{u_0 u_r i}{2nz} \tag{7}$$

D. Actuator Selection

Based on the biomechanics of the foot, an electric actuator is selected to simulate the tension force independently of the damping, thus allowing the rotation to be controlled during operation. Therefore, an actuator is needed that is light, fast, provides the necessary force and has a compact geometry due to limitations in the working area. The choice was the "Heavy Duty" linear actuator.

E. Assembly of the Prosthetic Prototype.

In view of the need to design a technological prototype that facilitates the integration of a patient with lower limb amputation, a standard model of prosthesis was chosen, innovated by electronic, mechanical and magnetic components. In addition, it incorporates weight and positioning sensors to give greater response and stability to a person's normal gait cycle, maintaining the primary characteristic of low cost. (Fig. 8) [18]

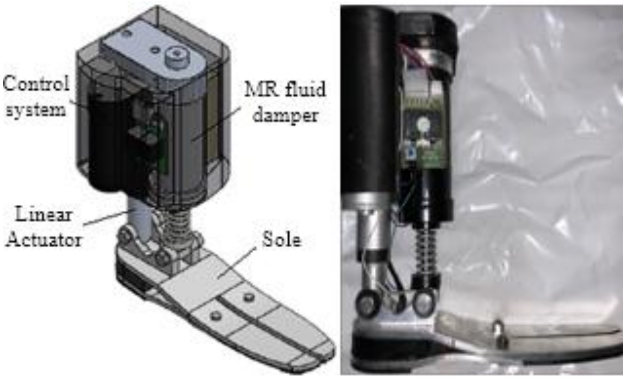

Figure 8. Assembly of the prototype of ankle and foot prosthesis.

F. Implementation of the Prosthetic Prototype

The prototype ankle-foot prosthesis consists of two main parts which are integrated to achieve the goal of a normal and efficient gait cycle; thus the first part is the control of the magnetorheological actuator whose function is the absorption of impacts during walking, while the second part is the control of the electric actuator intended to generate the dorsiflexion and planar flexion movements.

The damping force of the magnetorheological cylinder varies according to the weight supported by the prosthesis in each of the gait phases, so there are 3 load sensors, two FSR402 resistive sensors, one on the heel and the other on the sole of the prosthetic foot, as well as a 100kg Uxcell extensometer gauge between the two parts of the foot structure.

Once the data from the load sensors is acquired from the Arduino Nano controller board, the PWM signal is calculated and sent to the TB6612FNG motor driver, whose function is to vary the current intensity supplied to the magnetorheological actuator to control the damping distance according to the force required.

The movement of the prosthesis is generated by the extension and compression of the electric cylinder, which requires both the data acquired by the FSR402 resistive sensors and the value of the angle acquired by the MPU6050 accelerometer located at the top. The combinations between these variables in each phase of the walk are those that indicate the type of movement that the actuator must perform in order to meet the standards of normal walking.

All the electronic components are located on the left and right-side walls of the prosthesis, hidden under the casing made in 3D printing on thermoplastic elastomer material, to have an aesthetic and functional prototype, as shown in the Fig. 8.

III. Results

A. Magnetorheological Actuator Tests

To check the force that the magnetorheological cylinder is capable of withstanding, the actuator was subjected to a damper test to obtain graphical and numerical results corresponding to the compression and extension forces under the variation of the current intensity supplied to the magnetic induction system.

The results obtained on the Dyno-Shock 11 test stand for the current values of 0, 0.5, and 0.8 A are shown in Fig. 9. The force range in which the cylinder works within these three current values is 61.05 to 83.44 kg, so the controllable force of the actuator can be said to be 22.39 kg. It should be noted that the compression force is much greater than the extension force, because during the various tests the damping system was fully tested, i.e. the spring was coupled for the respective return to the cylinder.

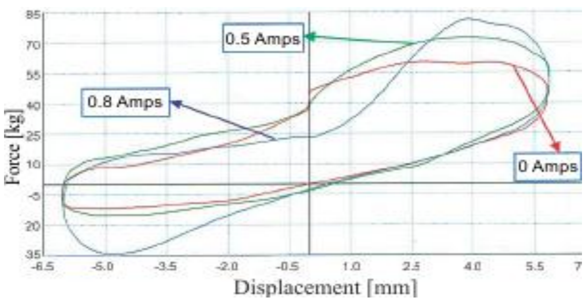

Figure 9. Force - Displacement Test.

B. Tests of Operation during the March.

The tests were carried out in a working space of 5 meters, as shown in Fig 10, in which 6 complete walking cycles are completed in a time of 8.14 seconds, thus determining the movement speed of 90 steps per minute which is very close to the average of 100 to 115 rpm. Fig. 10 shows the damping values of the prosthesis in each cycle, with respect to the distance where they are produced, obtaining an average stride length of 0.91m, which is less than the average of 1.50 metres but which can easily be increased according to the needs and maneuverability of the patient using the prosthetic prototype.

Figure 10. Damping point trajectory and values in running cycle.

In the test shown in Fig. 11 to measure the damping distance of the MR fluid damper piston during the gait cycle, it is determined that the values vary between 10 and 20 mm, with an average value of 15 mm, which is equal to the maximum stroke value Df calculated for the piston, obtaining a positive result due to the fact that it is within the permissible range according to the design carried out.

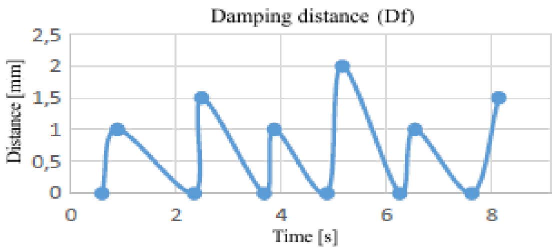

Figure 11. Damping graph.

Using the Kinovea software, experimental ankle angles were obtained in each of the gait cycles, obtaining values within a person's normal range of motion in dorsiflexion and planar flexion. Two of the most important aspects of the walk are speed and acceleration, which is why the values were obtained throughout the test trip, obtaining the results shown in Fig. 12 and 13.

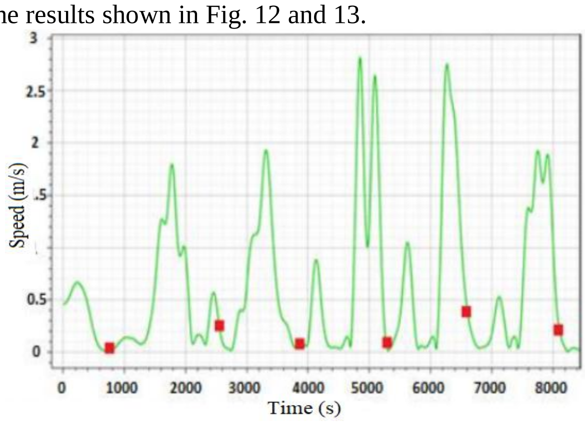

Figure 12. Prosthetic foot velocity chart.

The variation in the speed graph is due to the non-uniform walk that takes place during the test, since the prosthesis reacts according to the movements of the transtibial zone, therefore, the speed will depend directly on the individual, in this case the maximum speed reached is 2.8 m/s and takes place in the interval of 4.8 seconds, exactly during the change between the third and fourth cycle of the walk. In addition, acceleration is directly proportional to the speed so that its maximum value is given at the same instant of time reaching an equivalent of 24.5 m/s^2.

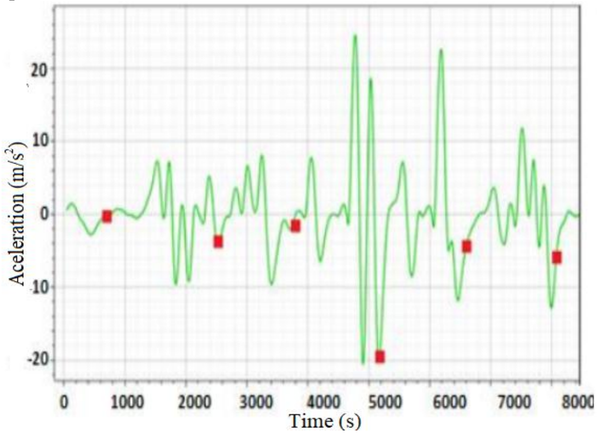

Figure 13. Acceleration chart of the prosthetic foot.

In Fig. 12 and 13, you can see the red cushioning points, the speed graph shows the decrease in the value when the prosthesis comes into contact with the ground and at that moment there is a deceleration that favors the absorption of impacts.

IV. Conclusions

The incorporation of magnetorheological fluids in the prototype allowed to obtain an improvement in the functionality of the foot and a significant cost reduction in relation to the existing prostheses in the market, taking as the most notable characteristics its quick response, its simple interface between the input of electrical energy and its mechanical output power, as well as its controllability and integration in the prosthetic system.

The mechanism successfully emulates the locomotion action during a walking cycle, since when the heel contacts the ground, the body's center of mass descends and the ankle tends to slow it down, an action represented by the magnetorheological system.

The use of the magnetorheological shock absorber in the ankle-foot prosthesis is appropriate, since it tends to stop the body's inertia produced during the initial contact of the heel with the ground, i.e. the prototype effectively fulfils the action of shock absorption and cushioning.

The prototype of ankle and foot prosthesis presents a passive and active functionality with a behavior very close to the normal walking cycle, achieving to offer a better comfort and an initiative of overcoming physiological, aesthetic and psychological problems that a disabled person presents.

The selection of the load sensors and the signal amplifier module was carried out correctly, as they met the response times required for proper data acquisition in real time.

By means of the scope achieved with the prototype of ankle and foot prostheses involving semi-active suspension systems, specifically the use of magnetorheological shock absorbers, the development of new technologies in our country can be generated and promoted, taking as a reference point the studies and advances already existing.

REFERENCES

[1] M. J. Espinoza and D. García, "Amputation Level In Lower Limbs: Impact On The Patient's Future Performance," *ScienceDirect,* p. 1, 2014.

[2] A. Lagares Alonso, M. Álvarez Salas, L. Garcés Pérez, L. Lérida Benitez and B. Romero Romero, "Musculoskeletal diseases associated with leg amputees," *ScienceDirect,* pp. 1-2, 2012.

[3] M. Tucker, "Control strategies for active lower extremity prosthetics and orthotics: a review," *Journal of NeuroEngineering and Rehabilitation,* pp. 4-6, 2015.

[4] J. Escalona and R. Torrealba, "Design of linear hydraulic actuator of variable response for intelligent knee prosthesis," *ResearchGate,* pp. 1-2, 2015.

[5] A. Simon, K. Ingraham and J. Spanias, "Delaying Ambulation Mode Transition Decisions Improves Accuracy of a Flexible Control System for Powered Knee-Ankle Prosthesis," *IEEE Transactions on Neural Systems and Rehabilitation Engineering* , vol. 25, n º8, pp. 1-2, 2017.

[6] F. Sup, A. Bohara and M. Goldfarb, "Design and Control of a Powered Transfemoral Prosthesis," *US National Library of Medicine* , pp. 1-2, 2009.

[7] P. Malcolm, R. Quesada, J. Caputo and S. Collins, "The influence of push-off timing in a robotic ankle-foot prosthesis on the energetics and mechanics of walking," *Journal of NeuroEngineering and Rehabilitation,* pp. 2-4, 2015.

[8] J. Rice and J. Schimmels, "Evaluation of a Two Degree of Freedom Passive Ankle Prosthesis with Powered Push-Off," *Journal of Medical Devices,* vol. 9, n º3, pp. 1-2, 2015.

[9] C. Mesquida and J. Lássig, "Introducción a los fluidos magnetoreológicos con aplicaciones en ingeniería," *Revista Iberoamericana de Ingeniería Mecánica,* vol. 16, n º1, pp. 22-36, 2012.

[10] M. Cupich and F. Elizondo, "Amortiguadores Magnetoreológicos," *Revista Ingenierías FIME-UANL,* vol. 1, n º2, p. 1, 1998.

[11] S. Mangal and V. Sharma, "On State Rheological Characterization of MRF 122EG Fluid Using Various Techniques," *ScienceDirect,* vol. 4, n º2, pp. 637-644, 2017.

[12] T. Avraam, "MR-fluid brake design and its application to a portable muscular rehabilitation device," *Semantic Scholar,* pp. 2-3, 2009.

[13] Lord Corporation, "MRF-140CG Magneto-Rheological Fluid," 2015. [On line]. Available: http://www.lordmrstore.com/lord-mr-products/mrf-140cg-magneto-rheological-fluid. [Último acceso: 15 07 2017].

[14] G. Singh Gohil and R. Srivastava, "Mechatronic design of Magneto-rheological damper for automobiles," *2013 Students Conference on Engineering and Systems (SCES),* vol. 1, n º1, 2013.

[15] F. D. Goncalves, M. Ahmadian and J. D. Carlson, "Investigating the magnetorheological effect at high flow velocities", Smart Materials and Structures, vol. 15, pp. 75–85, Dec. 2006.

[16] J. G. Chacón, A. Flórez and J. Rodríguez, "La inteligencia artificial y sus contribuciones a la física médica y la bioingeniería," *Revista MundoFesc,* vol. 1, n º9, pp. 60-63, 2015.

[17] R. G. Budynas and J. K. Nisbett, Shigley's mechanical engineering design, 10th ed, New York, United States of America: McGraw-Hill, 2015.

[18] F. Olmedo and F. Aguirre, "Diseño y simulación de una articulación de rodilla para prótesis externa usando herramientas CAD-CAE," *Sociedad Ibérica de Biomecánica y Biomateriales,* vol. 24, pp. 39-54, 2016.